

Dynamic simulations in the Model C universality class

Josh Ott

We present simulations of a non-conserved order parameter coupled to a conserved density at a critical point in the phase diagram. This model is the simplest realization of the Model C dynamic universality class in the Hohenberg and Halperin classification, which describes dynamic scaling for long-wavelength fluctuations near the QCD critical point. A Metropolis algorithm is used to solve for the dissipative dynamics of the model. After using the Binder cumulant method to find the critical temperature in 2 and 3 dimensions, we study correlation functions to extract the dynamic critical exponent z and observe strong and weak scaling regimes.

I. INTRODUCTION

In studying dynamic critical phenomena, there are many ways to extend models of static critical phenomena to include time dependence. These different approaches result in a selection of dynamic universality classes which share a common static universality class. Starting from the Ising static universality class corresponding to a d -dimensional magnet, one possible dynamical model involves imposing some structure with random anisotropy. In the standard classification scheme codified by Hohenberg and Halperin [1], this model is referred to as Model C. More specifically, Model C describes an N -component order parameter with relaxational dynamics, as in Model A, coupled to a conserved density with diffusive dynamics. On top of describing an Ising magnet with random anisotropy, it also describes a variety of other systems where a critical order parameter is coupled to a conserved density. One such system is found in the chiral order parameter of the QCD critical point [2].

The study of Model C has been approached both with perturbative and nonperturbative methods. Earlier work which utilized renormalization group and the ϵ expansion [3, 4] were limited to two-loop order by the complexities that come with including dynamic behavior. Motivated by the QCD phase transition, Model C in $2+1$ dimensions was studied through spectral functions [5] with classical-statistical simulation techniques. These simulations were used to determine the dynamic critical exponent z , though not to high precision. In addition, functional renormalization group has been used to study the phase diagram of Model C as a function of the dimension d and number of field components N [6]. It was shown that there are four regimes on this diagram corresponding to weak scaling, strong scaling, anomalous diffusion, and decoupled scaling. More recent work utilized a hybrid computational algorithm which simulated the dynamics of a lattice of Heisenberg spins in an external magnetic field [7].

In this work, we will apply a Monte Carlo method previously used to study the $O(4)$ critical point [8] to study Model C in the strong and weak scaling regimes. In particular, we consider an $N = 1$ component order parameter in $d = 2, 3$ dimensions. Based on previous work with functional renormalization group, we expect the weak scaling regime for $d = 2$ to exhibit two distinct

dynamic critical exponents for the order parameter and conserved density, respectively. For $d = 3$, we expect the strong scaling regime to exhibit “locking” of the dynamic critical exponents, where both fields experience the same scaling.

II. MODEL C

The equations of motion for Model C are given by

$$\frac{\partial \phi}{\partial t} = -\Gamma \frac{\delta \mathcal{H}}{\delta \phi} + \eta, \quad (1)$$

$$\frac{\partial \varepsilon}{\partial t} = \kappa \nabla^2 \frac{\delta \mathcal{H}}{\delta \varepsilon} + \zeta, \quad (2)$$

where we take the Hamiltonian to be

$$\mathcal{H} = \int d^d x \left\{ \frac{1}{2} (\nabla \phi)^2 + \frac{m^2}{2} \phi^2 + \frac{u}{4} \phi^4 + \frac{1}{2C_0} \varepsilon^2 + \frac{\gamma_0}{2} \varepsilon \phi^2 \right\}. \quad (3)$$

The first equation (1) describes the relaxational dynamics of an order parameter ϕ , and the second equation (2) describes the diffusive dynamics of a conserved density ε . One can interpret ε as being an energy density, for instance. The coefficients Γ and κ are the corresponding relaxation and diffusion rates, respectively. The fields η and ζ are delta-correlated Langevin noise sources with variance given by the fluctuation-dissipation relation

$$\langle \eta(t, \vec{x}) \eta(t', \vec{x}') \rangle = -2T\Gamma \delta(t-t') \delta(\vec{x}-\vec{x}'), \quad (4)$$

$$\langle \zeta(t, \vec{x}) \zeta(t', \vec{x}') \rangle = -2T\kappa \nabla^2 \delta(t-t') \delta(\vec{x}-\vec{x}'). \quad (5)$$

Note that we have let the \vec{x} - and t -dependence of the fields ϕ and ε be implied.

For simplicity, we set $u/4 = C_0 = \gamma_0 = \Gamma = \kappa = 1$ in our simulations. As we will be discretizing the model onto a lattice, we also use units such that the lattice spacing is $a = 1$.

III. NUMERICAL METHOD

To solve for the dynamics of Model C numerically, we discretize the theory onto a d -dimensional lattice of volume $V = L^d$. The Hamiltonian then gets discretized

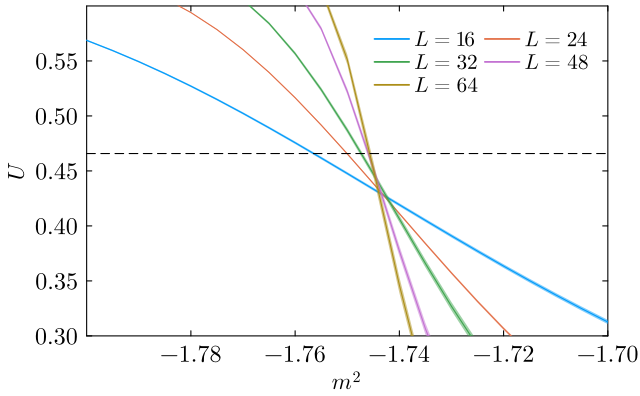


FIG. 1: Reweighted samples of the Binder cumulant performed around $m_0^2 = -1.74$ for various lattice sizes with bootstrapped error bars. The dashed line is the universal value of U^* at the critical point.

using forward derivatives

$$\mathcal{H} = \sum_{\vec{x}} \left\{ \frac{1}{2} \sum_{\hat{\mu}=1}^d (\phi(\vec{x} + \hat{\mu}) - \phi(\vec{x}))^2 + \frac{m^2}{2} \phi^2(\vec{x}) + \frac{u}{4} \phi^4(\vec{x}) + \frac{1}{2C_0} \varepsilon^2(\vec{x}) + \frac{\gamma_0}{2} \varepsilon(\vec{x}) \phi^2(\vec{x}) \right\}. \quad (6)$$

Following the work of Florio et al. [8], we use a Metropolis algorithm to simulate the dissipative Langevin dynamics of Model C. Since Model C has no non-vanishing Poisson brackets, it is unnecessary to employ the operator splitting approach since the equations are purely dissipative. In the basic Ising model case, the Metropolis algorithm works by proposing spin flips across the order parameter lattice. If the proposal lowers the energy of the system, the proposal is accepted without question. Otherwise, the proposal is rejected only with some probability. In our case, the order parameter is now real-valued, so we instead propose Gaussian-distributed trial updates to each site. For the order parameter, this proposal looks like

$$\phi(t + \Delta t, x) = \phi(t, x) + \sqrt{2\Delta t T \Gamma} \xi, \quad (7)$$

where ξ is a random number with zero mean and unit variance. The proposal is then accepted with probability $\min(1, e^{\Delta\mathcal{H}/T})$. This form is chosen such that the mean of this update reproduces the dissipative term

$$\langle \phi(t + \Delta t) - \phi(t) \rangle = -\Delta t \Gamma \frac{\delta \mathcal{H}}{\delta \phi} + \mathcal{O}(\Delta t^2) \quad (8)$$

and the variance reproduces the stochastic term

$$\langle (\phi(t + \Delta t) - \phi(t))^2 \rangle = 2\Delta t T \Gamma. \quad (9)$$

For the conserved density, more care is required. Rather than proposing updates to each site individually,

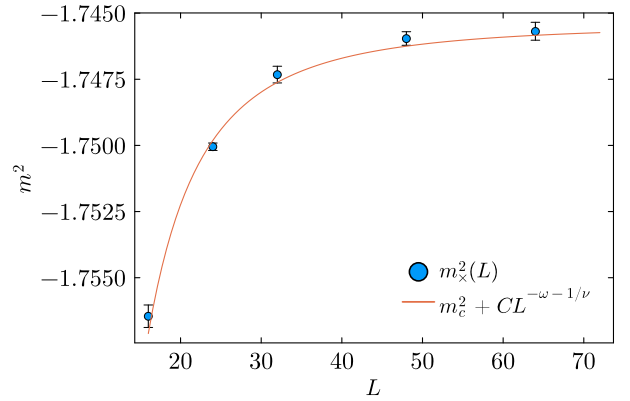


FIG. 2: Scatter plot of the intersection points of the reweighted Binder cumulants from Fig. 1 with U^* along with a fit to the expected L -dependence from finite scaling. Error bars are taken directly from the error bars in Fig. 1

we consider adjacent pairs of sites and propose equal and opposite updates. That is, for some unit vector $\hat{\mu}$, we propose

$$\varepsilon(t + \Delta t, \vec{x}) = \varepsilon(t, \vec{x}) + \sqrt{2\Delta t T \kappa} \xi, \quad (10)$$

$$\varepsilon(t + \Delta t, \vec{x} + \hat{\mu}) = \varepsilon(t, \vec{x} + \hat{\mu}) - \sqrt{2\Delta t T \kappa} \xi. \quad (11)$$

This ensures that the field ε is conserved and that fluctuations can only travel locally. Since there are d choices for the unit vector $\hat{\mu}$, this updating ε is slower than updating ϕ by a factor of d .

Individual Metropolis steps can be sped up by parallelizing the sweeps across lattice sites. For the order parameter, we do this using a checkerboard pattern to avoid race conditions arising from the gradient term in the Hamiltonian. For the conserved density, a checkerboard pattern is also required due to the interactions with adjacent sites that come from the conservation requirement.

IV. LOCATING A CRITICAL POINT

The critical value of m^2 that results in a scale-invariant Hamiltonian is not universal and thus must be determined from simulations. We can accomplish this by taking advantage of properties which are indeed universal using the Binder cumulant method. This method rests on the observation that the Binder cumulant

$$U = 1 - \frac{\langle M^4 \rangle}{3\langle M^2 \rangle^2} \quad (12)$$

has finite volume corrections which cancel at the true critical temperature m_c^2 . Here, the magnetization M is defined as

$$M = \int d^d x \phi(\vec{x}). \quad (13)$$

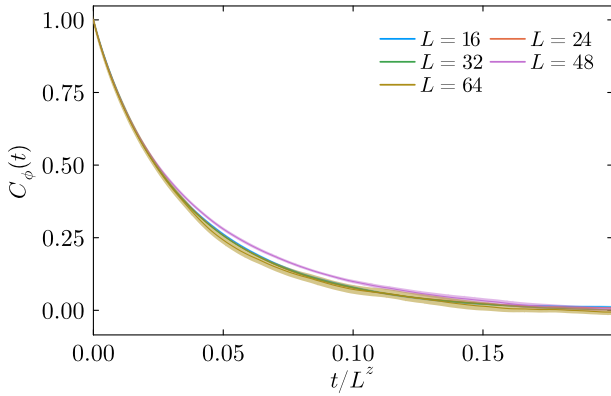


FIG. 3: Correlation functions $C_\phi(t)$ of ϕ in 3 dimensions shown with data collapse for $z = 2.10$.

In particular, we compute the Binder cumulant at various lattice sizes and look for the temperature $m_\times^2(L)$ at which it crosses a universal value U^* as a function of the lattice side length L . Finite size scaling predicts that the intersection point will be of the form

$$m_\times^2(L) = m_c^2 + CL^{-\omega-1/\nu} \quad (14)$$

for some constant C . The critical temperature can then be extracted from a simple fit to the data.

In practice, it would be quite computationally expensive to gather data for a dense selection of temperatures around m_c^2 . It is easier to perform a coarse search to narrow down a single candidate temperature and then perform the fit using reweighted samples. Reweighting comes from the simple manipulation

$$\langle \mathcal{O} \rangle = \frac{\int \mathcal{D}\phi \mathcal{O} e^{-\delta\mathcal{H}} e^{-\mathcal{H}_0}}{\int \mathcal{D}\phi e^{-\delta\mathcal{H}} e^{-\mathcal{H}_0}} = \frac{\langle \mathcal{O} e^{-\delta\mathcal{H}} \rangle_0}{\langle e^{-\delta\mathcal{H}} \rangle_0} \quad (15)$$

where $\mathcal{H} = \mathcal{H}_0 + \mathcal{H}_*$ and $\langle \cdot \rangle_0$ denotes averaging with respect to \mathcal{H}_0 . If we perform simulations at some m_0^2 , then we can get reweighted samples at $m_0^2 + \delta m^2$ with $\delta\mathcal{H} = \frac{\delta m^2}{2} \sum_{\vec{x}} \phi(\vec{x})^2$.

We will now use this method to determine the critical temperature of Model C in $d = 3$ dimensions. We use the exponents $\nu = 0.62999(5)$ and $\omega = 0.8303(18)$, which were determined in [9]. The universal value of the Binder cumulant $U^* = 0.4658$ was determined in [10].

After an initial survey of temperatures, we perform reweighting around $m_0^2 = -1.74$. The resulting curves are shown in Fig. 1. The intersection points $m_\times^2(L)$ of the reweighted samples with the universal value as a function of L can then be extracted, and we find the resulting data falls nicely onto the expected form predicted by finite size scaling. A fit to this form yields the critical temperature $m_c^2 = -1.7454(2)$ in the infinite volume limit.

Next, we perform the same procedure in $d = 2$ dimensions. Here, the relevant exponents are precisely $\nu = 1$ and $\omega = 2$. The universal value of the Binder cumulant

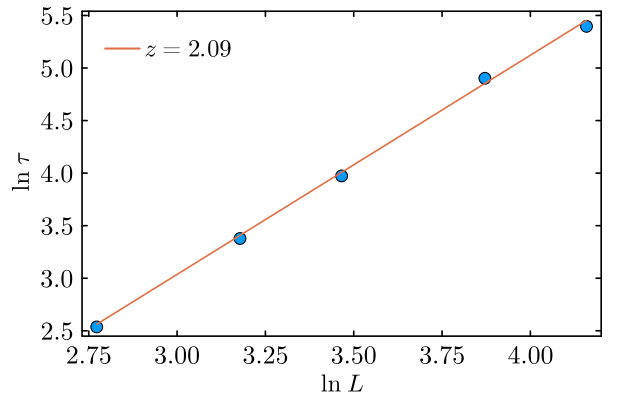


FIG. 4: Relaxation times of ϕ plotted for various lattice sizes in $d = 3$, with a fit to the form $\tau \sim L^z$ to extract the dynamic critical exponent. The orange line shows $z = 2.09$.

was measured to be $U^* = 0.61069$ using Monte Carlo methods in [11].

Again, a rough sweep through temperatures informs a choice of $m_0^2 = -3.52$. Reweighting was then performed for $L = 16, 24, 32, 40, 48, 64$. Unlike in 3 dimensions however, the expected L dependence did not hold for the lowest lattice sizes. This could be because a 16^2 lattice is in some sense “smaller” than a 16^3 lattice, so subleading finite size corrections become important for $L = 16$ in 2 dimensions where they did not in 3 dimensions. We restrict to the region where $m_\times^2(L)$ is strictly monotonic by only considering $L \geq 32$ and obtain $m_c^2 = -3.524(1)$.

Due to the failing of our finite size scaling prediction to explain the smallest lattices, it is likely that the error bars from the fit do not tell the whole story. Reweighting at several different m_0^2 in the vicinity of our result consistently pointed toward ~ -3.52 , however, so a more accurate error estimate would be $m_c^2 = -3.524(9)$. For our simulations at the critical point, we choose to set $m_c^2 = -3.524$.

V. RESULTS

To extract the dynamic critical exponent z at the critical point, we work with correlation functions of the fields ϕ and ε in Fourier space

$$\phi(\vec{k}) = \sum_{\vec{x}} \phi(\vec{x}) e^{i\vec{x}\cdot\vec{k}}, \quad \varepsilon(\vec{k}) = \sum_{\vec{x}} \varepsilon(\vec{x}) e^{i\vec{x}\cdot\vec{k}}. \quad (16)$$

On the lattice, wave numbers are discretized as $\vec{k} = 2\pi\vec{n}/L$ where $n_i = 0, \dots, N - 1$. The correlation function of the order parameter is defined as

$$C_\phi(t, \vec{k}) = \left\langle \phi(0, \vec{k}) \phi(t, -\vec{k}) \right\rangle \sim \exp(-t/\tau) \quad (17)$$

where τ is the relaxation time. At the critical point, the correlation length ξ is limited by the side length fo

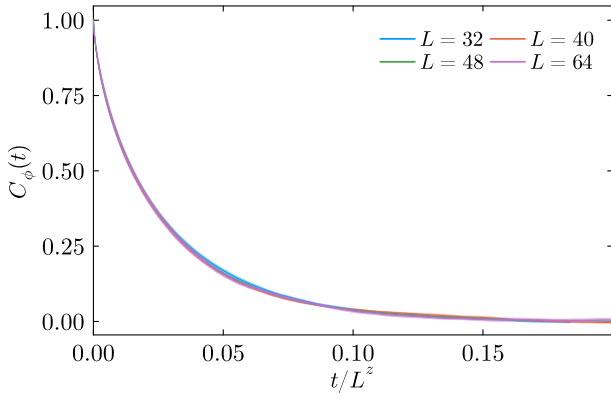


FIG. 5: Correlation functions of ϕ in 2 dimensions shown with data collapse for $z = 2.36$.

the lattice L , and the relaxation time scales as $\tau \sim L^z$. We thus perform simulations at m_c^2 at several lattice sizes and save $\phi(t, \vec{k})$ for many t . By extracting τ for each L , we can perform a fit to extract z . The correlation function for the conserved density $C_\varepsilon(t, \vec{k})$ is defined identically, with its own dynamic critical exponent z_ε .

We first extract the dynamic critical exponent z for the order parameter as well as the exponent z_ε for the conserved density in $d = 3$ dimensions. Using our simulations, we time evolve the system at m_c^2 and regularly save the $k = 2\pi/L$ mode of both $\phi(\vec{k})$ and $\varepsilon(\vec{k})$. From multiple of these runs, we can compute $C_\phi(t) \equiv C_\phi(t, 2\pi/L)$ and $C_\varepsilon(t)$, normalizing such that $C(0) = 1$. The resulting curves are shown in Fig. 3. We then assume these curves take the form $C(t) \sim e^{-t/\tau}$ and fit the value of τ . Finally, we can plot $\ln \tau$ vs $\ln L$ and perform a linear fit to get z , as shown in Fig. 4. We find $z = 2.09$, in good agreement with the value $z = 2.069$ found in [6]. Error is difficult to estimate since very little uncertainty is reported in the linear fit. Much of the uncertainty indeed comes from the determination of m_c^2 .

We also perform the same analysis with $C_\varepsilon(t)$ and find

$z_\varepsilon = 2.10$, in strong agreement with the expectation that the two dynamic critical exponents coincide in the strong scaling regime.

Finally, we turn to 2 dimensions, where we expect z and z_ε to no longer coincide. To account for this, simulations are performed assuming $z = 2.4$ to ensure the fields are given sufficient time to evolve. The collapsed correlation functions ϕ are shown in Fig. 5 for the extracted value $z = 2.36$. Repeating this analysis for the conserved density, we now find $z_\varepsilon = 2.13$, clearly signaling the emergence of two distinct time scales in 2 dimensions.

VI. CONCLUSION

We have demonstrated the effectiveness of the Metropolis algorithm approach to simulating Model C by studying correlation functions near the critical point and observing strong and weak scaling regimes in 3 and 2 dimensions, respectively. For $d = 3$ we find $z = 2.09$ and $z_\varepsilon = 2.10$, in good agreement with previous work which used functional renormalization group. For $d = 2$, we find $z = 2.36$ and $z_\varepsilon = 2.13$.

This work would certainly benefit from more time to gain statistics: even these rough simulations took several days of compute time on a cluster. Even with sparse statistics, however, the characteristics of Model C still came through. The real benefit of this method, however, is the control one has over the parameters of the system to study truly nonperturbative phenomena. The main limiting factor is finite size effects. For this work, only CPUs were used, but taking advantage of GPUs would allow for larger, finer lattices.

Acknowledgments

I would like to thank Mehran Kardar for a delightful semester of statistical mechanics, and Vladimir Skokov for useful discussions.

-
- [1] P. C. Hohenberg and B. I. Halperin, *Rev. Mod. Phys.* **49**, 435 (1977).
 - [2] B. Berdnikov and K. Rajagopal, *Phys. Rev. D* **61**, 105017 (2000), [arXiv:hep-ph/9912274](#).
 - [3] M. Dudka, R. Folk, Y. Holovatch, and G. Moser, *Journal of Physics A: Mathematical and Theoretical* **40**, 8247–8264 (2007).
 - [4] R. Folk and G. Moser, *Phys. Rev. Lett.* **91**, 030601 (2003).
 - [5] J. Berges, S. Schlichting, and D. Sexty, *Nucl. Phys. B* **832**, 228 (2010), [arXiv:0912.3135 \[hep-lat\]](#).
 - [6] D. Mesterházy, J. H. Stockemer, L. F. Palhares, and J. Berges, *Phys. Rev. B* **88**, 174301 (2013), [arXiv:1307.1700 \[cond-mat.stat-mech\]](#).
 - [7] R. Nandi and U. C. Täuber, *Phys. Rev. E* **102**, 052114 (2020), [arXiv:2008.11541 \[cond-mat.stat-mech\]](#).
 - [8] A. Florio, E. Grossi, A. Soloviev, and D. Teaney, *Phys. Rev. D* **105**, 054512 (2022), [arXiv:2111.03640 \[hep-lat\]](#).
 - [9] S. El-Showk, M. F. Paulos, D. Poland, S. Rychkov, D. Simmons-Duffin, and A. Vichi, *J. Stat. Phys.* **157**, 869 (2014), [arXiv:1403.4545 \[hep-th\]](#).
 - [10] M. Hasenbusch, K. Pinn, and S. Vinti, (1998), [arXiv:cond-mat/9804186](#).
 - [11] W. Selke and L. N. Shchur, *Phys. Rev. E* **80**, 042104 (2009), [arXiv:0906.0721 \[cond-mat.stat-mech\]](#).